LASER PHYSICS LETTERS

www.lphys.org

WILEY-VCH

Abstract: We have measured light shifts, also known as AC Stark shifts, as a function of laser intensity in cold Rubidium atoms by observing sub-natural linewidth gain and loss features in the transmission spectrum of a weak probe beam passing through the atomic sample. The observed energy-level shifts for atoms in a magneto-optical trap (MOT) are found to be consistently higher than that obtained in optical molasses (i.e., when the magnetic field gradient in the MOT is turned off). Using a simple model of a multilevel Rubidium atom interacting with pump and probe beams, we have calculated the theoretical light shift as a function of intensity. A comparison of these calculated values with the light shift data obtained for molasses reveals good agreement between experiment and theory. Further, our model elucidates the role of the Zeeman shifts arising from the magnetic field gradient in the observed probe transmission spectrum for the MOT.

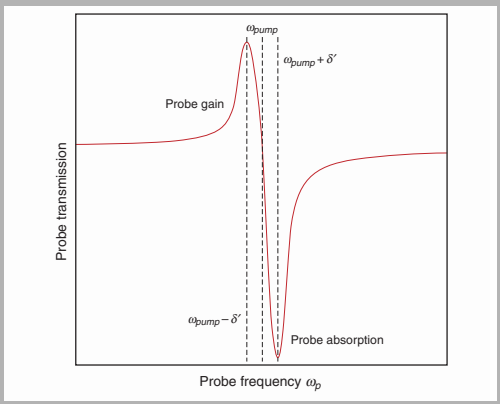

A qualitative plot of the transmission spectrum of a probe beam through a fictitious sample of cold $J=1 \rightarrow J'=2$ atoms showing probe absorption at the sum of the pump frequency ω_{pump} and δ', where δ' is the difference of the light shifts between the $|J=1,m_J=0\rangle$ and the $|J=1,m_J=\pm 1\rangle$ ground state Zeeman sublevels. Probe gain is depicted at $\omega_{pump}-\delta'$. See Fig. 3 and accompanying text for further explanation

Measurements of light shifts in cold atoms using Raman pump-probe spectroscopy

N. Souther, R. Wagner, P. Harnish, M. Briel, and S. Bali *

Department of Physics, Miami University, Oxford, OH 45056, USA

Received: 13 November 2009, Revised: 22 November 2009, Accepted: 25 November 2009
Published online: 8 February 2010

Key words: Raman spectroscopy; pump-probe spectroscopy; light shift; AC Stark shift; optical molasses; magneto-optical trap

PACS: 32.30.-r, 32.60.+i, 32.70.-n, 32.70.Fw, 32.70.Jz, 37.10.De, 42.50.Hz, 42.62.Fi

1. Introduction

Pump-probe atomic spectroscopy refers to the widely used technique of allowing two beams of light to be simultaneously incident on an atomic sample: one, a strong, fixed-frequency pump beam that induces interesting dynamics we wish to study, and the other, a weak probe beam that is scanned in frequency around that of the pump. By examining frequency-dependent probe absorption or amplification, arising from Raman transitions between the atomic states, we may investigate the pump-induced atomic dynamics. In the context of cold atoms, the use of Raman pump-probe spectroscopy to extract information on the rich and varied dynamics of atoms confined in optical lattices was pioneered by G. Grynberg and C. Robilliard [1]. More recently W. Gawlik and collaborators have demonstrated the use of Raman pump-probe spectroscopy to study anisotropy of the momentum distribution in an operating magneto-optical trap (MOT) [2,3].

D. Grison, et al. [4] and J.W.R. Tabosa, et al. [5] were the first to observe narrow, sub-natural linewidth Raman transitions occurring between light-shifted Zeeman sub-

* Corresponding author: e-mail: balis@muohio.edu

levels of cold trapped atoms. The observation of gain in the probe transmission spectrum [4,5] demonstrated the existence of significant population differences among the various Zeeman ground-state atomic sublevels, thus validating important sub-Doppler laser cooling models that had just been developed at that time [6]. In [5] this probe gain was used to create negative radiation pressure in the trapped sample. A few years later the dependence of probe gain and loss on various polarization configurations of the pump and probe fields was systematically investigated [7].

It is surprising that, despite all this attention to pump-probe spectroscopy of Raman transitions between light-shifted Zeeman sublevels, no-one has yet reported an explicit measurement of the intensity dependence of the light shifts in the Zeeman sub-levels of cold atoms and compared these measurements with theoretical predictions. Previous workers have confirmed a linear scaling of the light shift for low intensities which segues into a square-root scaling as the intensity rises [4,8], in accordance with theory. However, discrepancies between data and theory still exist in the form of an offset between the observed and calculated curves, arising from the presence of extraneous frequency-shifts caused by residual magnetic fields, or due to unresolved errors in the determination of the true intensity at the site of the cold atoms. Previous workers have noted this discrepancy between data and theory, and have in fact used the light-shift measurement to extract the correct value of the intensity [9], or the average Rabi frequency [8]. It is important to understand and eliminate such discrepancies and unaccounted frequency-shifts in cold atom measurements because an increasing number of researchers use the MOT as a convenient starting point for a variety of novel and elegant spectroscopic measurements, such as recoil ion momentum spectroscopy (see, for example [10]), and measurements of recoil-induced Raman resonances in optical lattices [11] and highly anisotropic optically thick MOT's [12]. Light shifts in a Bose-Einstein condensate (BEC) have also been measured recently using matter-wave interferometry [13], where the observed line-broadening yields information on collective scattering effects, which are of importance in BEC theory (see, for example [14]) and experiment (see, for example [15]).

In this letter we demonstrate the use of Raman pump-probe spectroscopy to explicitly measure the intensity dependence of the light shift in cold Rubidium atoms. The level-shifts for atoms in an operating MOT are observed to be consistently higher than that obtained in optical molasses (obtained by turning off the magnetic field gradient in the MOT). In order to compare these measurements with theory we develop a simple model of a multilevel Rubidium atom interacting with pump and probe beams and calculate the theoretical light shift as a function of intensity. A comparison of these calculated values with the light shift data obtained for molasses reveals good absolute agreement between experiment and theory. It is clear that in the case of the MOT there are additional Zeeman shifts that obfuscate the light shift measurement. The role of the Zeeman shifts in the observed Raman pump-probe spectrum for the MOT is elucidated.

2. Theoretical model for light shifts in ^{85}Rb

The calculation of the light shift for a two-level atom is well known [16]. Assuming a $\mathbf{d}\cdot\mathbf{E}$ light-atom interaction, where $\mathbf{E}$ is the incident electromagnetic field and $\mathbf{d}$ is the induced atomic dipole, one uses the Schrodinger equation in the rotating wave approximation for the dressed atomic wavefunction

$$|\Phi(t)\rangle = c_g(t)|g\rangle + c_e(t)|e\rangle$$

(where $|g\rangle$ ($|e\rangle$) is the ground (excited) state of the two-level atom, and c_g (c_e) is the probability amplitude of the atom being found in this state) to obtain the coupled differential equations

$$i\dot{c}_g = -\frac{\chi^*}{2}\,c_e \quad \text{and} \quad i\dot{c}_e = \Delta c_e - \frac{\chi}{2}\,c_g\,,$$

which are solved to obtain the ground state energy value

$$E_g = \frac{\hbar}{2}\left(\Delta - \sqrt{\Delta^2 + |\chi|^2}\right)\,. \tag{1}$$

Here χ is the Rabi frequency, and Δ is the detuning $\Delta \equiv \omega_{eg} - \omega_L$ of the incident laser frequency ω_L from the atomic resonance frequency ω_{eg}. Prior to interacting with the incident light field the energy of the ground state was, by definition, zero. Hence Eq. (1) represents the light shift δ_{LS}, also known as the AC Stark shift, in the ground state of the two-level atom owing to the incident light.

If we turn our attention now from a two-level atom to a real multilevel atom we need to take into account the relative strength of the different transitions. In our case, the transitions of interest are the Zeeman sublevels of the hyperfine transition $F = 3 \leftrightarrow F' = 4$ in ^{85}Rb. The light shift, in units of frequency, for any one of the Zeeman ground states m_F ($-3 \le m_F \le 3$) is now given by

$$\frac{1}{\hbar}(\delta_{LS})_{m_F} = \frac{\Gamma}{2}\left(\frac{\Delta}{\Gamma} - \sqrt{\frac{\Delta^2}{\Gamma^2} + \frac{I}{2I_{sat}}}\right)\left|c_{m_F m_{F'}}\right|^2\,, \tag{2}$$

where we have incorporated into Eq. (1) the Clebsch-Gordan coefficient $c_{m_F m_{F'}}$ for the transition between the ground state m_F and the excited state $m_{F'}$, and for convenience written the Rabi frequency χ in terms of measurable quantities I (laser intensity) and I_{sat} (the saturation intensity for the hyperfine transition) via the relation $I/I_{sat} \equiv 2|\chi|^2/\Gamma^2$, Γ being the natural linewidth for the transition. For the $F = 3 \leftrightarrow F' = 4$ transition in ^{85}Rb $I_{sat} = 1.64$ mW/cm^2 and $\Gamma/2\pi = 5.98$ MHz. The squared-values of the Clebsch-Gordan (CG) coefficients for all possible transitions between the Zeeman sublevels of the $F = 3 \leftrightarrow F' = 4$ transition in ^{85}Rb are shown in Fig. 1a.

The squares of the CG coefficients for each Zeeman sublevel in the ground state, and hence the relative size of

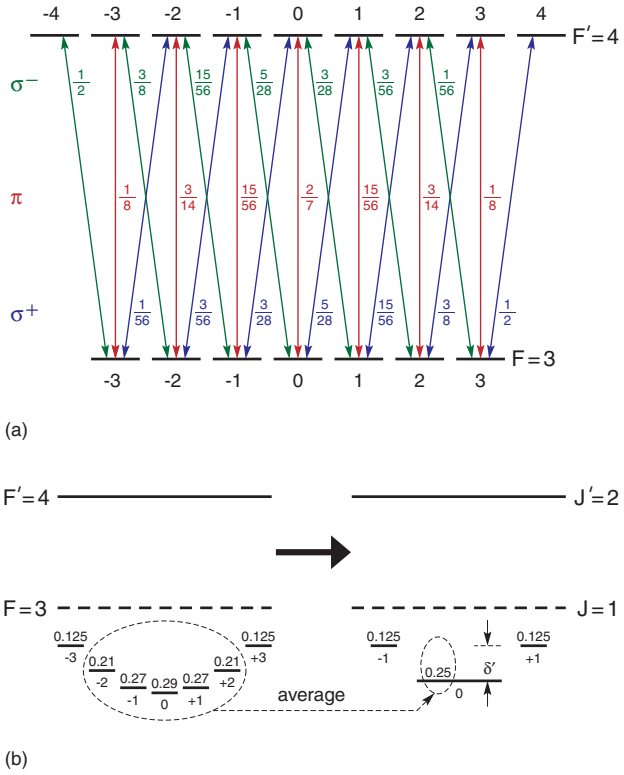

Figure 1 (online color at www.lphys.org) (a) Values of the squared Clebsch-Gordan (CG) coefficients for all possible transitions between the Zeeman sublevels of the $F=3 \leftrightarrow F'=4$ transition in ^{85}Rb. (b) Modeling the Rb atom as a fictitious $J=1 \leftrightarrow J'=2$ system. See text for further explanation

the light shift for each sublevel, are shown in Fig. 1b. One may approximate the five close-lying ground states, shown encircled in Fig. 1b, as one (with an average squared-CG coefficient of 0.25), effectively modeling the Rb atom as a $J=1 \rightarrow J'=2$ system. For this system the relative light shift between the ground states is denoted by δ' as shown in Fig. 1b. The value of δ' is calculated by first substituting 0.25 for the value of $|c_{m_F m_{F'}}|^2$ in Eq. (2) in order to determine the light shift of the lowest Zeeman sublevel, and then substituting 0.125 in order to determine the light shift of the upper ground state sublevels, and taking the difference of the two light shifts, i.e.,

$$\delta' \equiv \left(\delta_{LS}\right)_{m_F=0} - \left(\delta_{LS}\right)_{m_F=\pm 1} . \qquad (3)$$

3. Experimental setup

A detailed description of the setup can be found in [17]. Here, we only present the relevant details. Our experiment uses a standard vapor-loaded $\sigma^+ - \sigma^-$ ^{85}Rb magneto-optical trap in a stainless-steel vacuum chamber with anti-reflection coated windows. The 780-nm light from an external cavity tunable diode laser (see Fig. 2) that is locked to a hyperfine atomic transition using saturated absorption spectroscopy, is divided into three mutually orthogonal beams (not shown), each of which is retroreflected.

The sum of all six trapping beams (15 mm in diameter) at the position of the cold atoms is typically several mW/cm^2 and can be varied with half-wave plate H2 (see Fig. 2). A much weaker repumping light beam is added to prevent the atoms from accumulating in the lower hyperfine $F=2$ ground state. A pair of current-carrying coils external to the vacuum chamber provide an axial magnetic field gradient of 12 G/cm. Three other pairs of current coils are placed in Helmholtz configuration around the vacuum chamber in order to cancel dc magnetic fields at the site of the cold atom cloud. The temperature of the cold atoms is typically $30-50$ μK.

In order to detect sub-MHz features using pump-probe spectroscopy the pump and probe beams are derived from the same laser [4] to preserve the requisite phase coherence. The trapping beams themselves serve as the pump. As shown in Fig. 2 a frequency-scannable probe beam is prepared by passing a small portion of the laser beam through an acousto-optic modulator AO1, and aligning the frequency-shifted first-order output from AO1 through a second acousto-optic modulator AO2 in scanning-mode (i.e., a continuously ramping voltage is applied to the "tuning" input of its driver). The first-order output of AO2 forms the probe beam. The first-order outputs of AO1 and AO2 are chosen to be of opposite sign so that the probe beam frequency is centered on the original laser (pump) frequency, but now is capable of scanning around it. The acousto-optic modulator AO2 (and also AO1) is operated in "double-pass" mode because it is important that the frequency-scanning probe beam stays centered on the cold atom cloud and does not move spatially as its frequency is swept back and forth. The probe polarization and intensity is adjusted with a $\lambda/2$ plate-polarizer combination (H5 and P in Fig. 2), and then focused with lens L3 down to a spot of 0.4 mm diameter at the center of the cold atom cloud (diameter 2.3 mm), with a Rayleigh range much longer than the cloud diameter. The probe beam is linearly polarized. The frequency of the probe beam is scanned at 1.8 MHz/ms for a period of 3.3 ms around the pump frequency (which is held fixed at a detuning of -2.5Γ from atomic resonance). The pump intensity (measurement described in the following Section) ranged from 4.5 to 9 mW/cm^2 while the probe intensity ranged from 0.03 to 0.5 mW/cm^2. At this detuning and intensity the probe is too weak to visibly exert any forces on the atoms, and is therefore allowed to always be incident on the atomic cloud. The $\lambda/2$-beamsplitter combination (H6 and PBS4 in Fig. 2) is used to split the probe into two beams of equal intensity, one of which passes through the cold atoms while the other passes close to the atoms but not through them. The two beams are allowed to fall onto a pair of photodiodes whose outputs are subtracted in order to eliminate technical noise in the probe laser beam. The transmission spectrum of the probe is amplified and observed on an os-

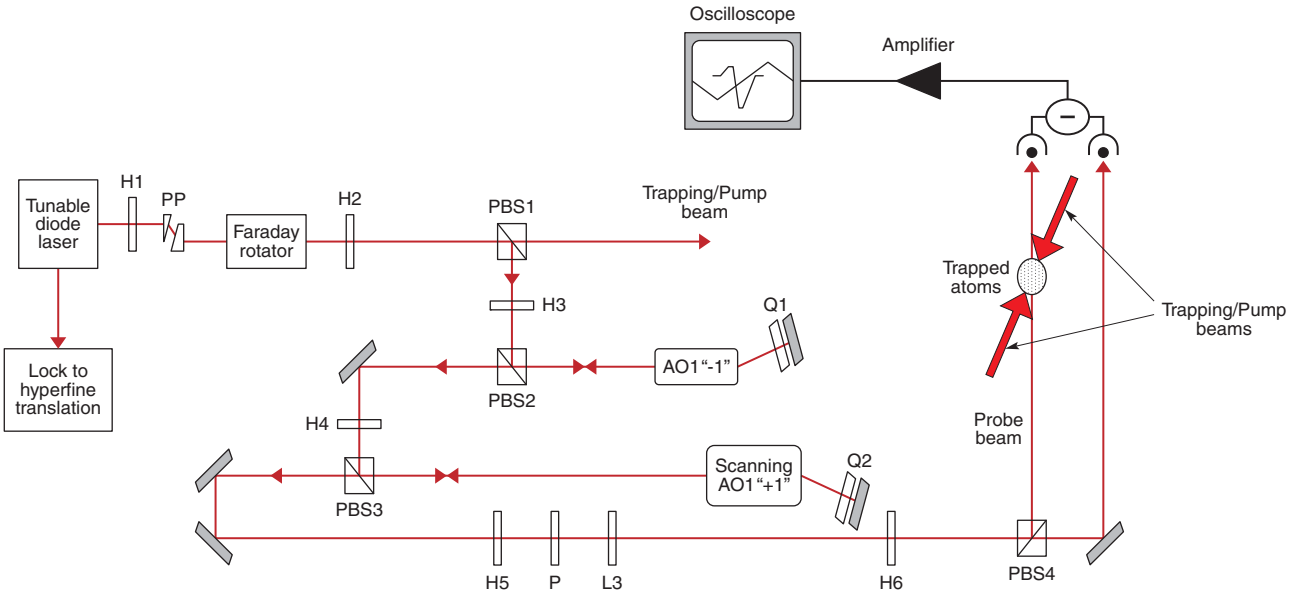

Figure 2 (online color at www.lphys.org) Setup of our experiment to measure light shifts in cold atoms using Raman pump-probe spectroscopy. L: lens; P: polarizer; PBS: polarizing beam splitter; H: half-wave plate; Q: quarter-wave plate; PP: prism pair for circularizing laser beam; AO: acousto-optic modulator

cilloscope. A typical transmission spectrum for the probe beam is shown in Fig. 3a.

Transmission spectra are recorded for atoms in the MOT as well as in optical molasses. In the case of molasses, the trapping magnetic field gradient is first turned off and a 1-2 ms delay allowed for the atoms to thermally equilibrate before initiating the frequency scan of the probe beam. After the scan is completed the magnetic field gradient is turned back on and the cold atom trap is reloaded for 1 sec. The process above is then repeated. The data shown in Fig. 3a is an average over several (typically 5 – 10) scans.

4. Data and discussion

In the simplest pump-probe measurement scheme of the light shift, there is a single strong pump beam that creates the light shifts, and a weak probe beam that extracts information about the atomic population distribution without affecting the environment created for the atoms by the pump. The pump is fixed in frequency, while the probe beam is frequency-scanned around the pump. In our case, the six $\sigma^+ - \sigma^-$ MOT beams act as the pump beams and the probe is a weak linearly polarized external beam that propagates almost collinearly with a pair of the MOT beams.

As shown in Fig 3a, probe gain and absorption is observed when the probe is displaced on either side of the pump frequency by the difference δ' of light shifts between the ground state Zeeman sublevels. This displacement is perfectly symmetrical for a fictitious $J = 1 \leftrightarrow J' = 2$ but slightly asymmetrical for real $F = 3 \leftrightarrow F' = 4$ Rb atoms. In keeping with the spirit of our simple model we define the frequency separation between the probe-gain and probe-loss features to be twice the value of δ'. We explain the probe gain and absorption features in terms of stimulated Raman transitions between the light-shifted Zeeman ground sub-levels [4], as shown in Fig. 3b, Fig. 3c, and Fig. 3d.

Let's consider the action on a $J = 1 \leftrightarrow J' = 2$ model system (see Fig. 1b) of pump light with fixed frequency ω_{pump} and a probe beam with variable frequency ω_{probe}, both of which are red-detuned from resonance with the excited state. Because the pump is formed by counter-propagating circularly-polarized MOT beams the atoms see a net linear polarization that rotates in space [6]. Just as in the standard treatment of sub-Doppler cooling [6] with $\sigma^+ - \sigma^-$ trapping beams it is convenient to switch to the reference frame of the helically rotating polarization so that the pump beam has a fixed linear polarization. However, now the probe beam has π, σ^+, and σ^- components. We show below that, in conjunction with the π-polarized pump, the σ^+ and σ^- components of the probe give rise to Raman transitions between the light-shifted levels as depicted in Fig. 3b, Fig. 3c, and Fig. 3d. The π-polarized component of the probe cannot cause a transfer of population from one ground-state sublevel to another in this model system.

A cursory glance at the Clebsch-Gordan coefficients in Fig. 1 reveals that the atomic population predominantly resides in the lowest ground-state sublevel. When

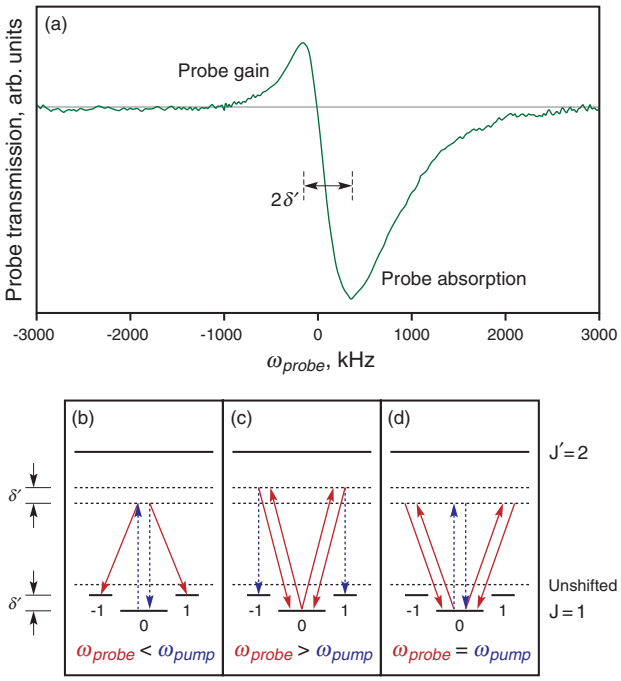

Figure 3 (online color at www.lphys.org) (a) Observed probe transmission spectrum. In Figs. (b), (c), and (d) the probe (pump) is denoted by solid (dashed) lines. (b) $\omega_{probe} < \omega_{pump}$: absorption from the pump, followed by stimulated emission into the probe, leads to probe gain. (c) $\omega_{probe} > \omega_{pump}$: absorption from the probe, followed by stimulated emission into the pump, leads to probe loss. (d) $\omega_{probe} = \omega_{pump}$: neither probe gain nor probe loss is observed

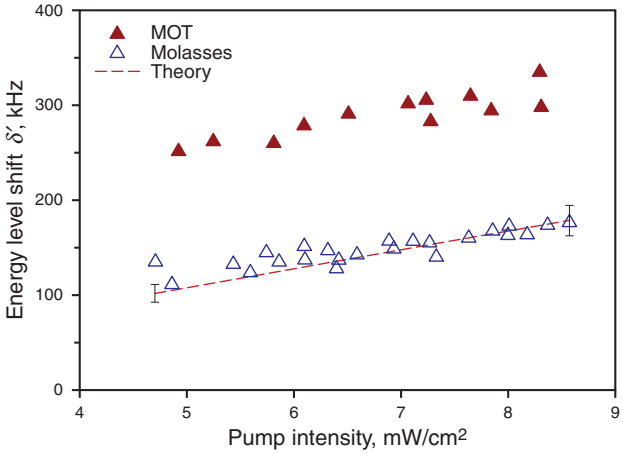

Figure 4 (online color at www.lphys.org) Measurement of the light shifts for molasses, and a combination of light shifts and Zeeman shifts for the MOT. The theoretical line is obtained from Eq. (2) with no free parameters. The error bars on the theoretical curve, shown on just the two end-points of the curve, reflect the experimental uncertainty in our knowledge of the pump detuning (see text)

$\omega_{probe} < \omega_{pump}$, the pump is closer to resonance with the excited state and thus is far more likely than ω_{probe} to excite the atoms from the $|1,0\rangle$ state to the excited state (i.e., to the $|2,0\rangle$ state because ω_{pump} is π-polarized) and then, by stimulated emission back into the pump, to the $|1,0\rangle$ state again. However, as ω_{probe} approaches the value $\omega_{pump} - \delta'$ the excited atoms are increasingly induced by the σ^+ and σ^- components of the probe to make a stimulated emission into the probe beam and drop from $|2,0\rangle$ to the $|1,\pm1\rangle$ ground states (see Fig. 3b). This absorption from the pump followed by stimulated emission into the probe causes a gain in the transmitted probe power, as shown in Fig. 3a. Note that the probe gain is maximum when $\omega_{probe} = \omega_{pump} - \delta'$.

On the other hand, as ω_{probe} becomes larger than ω_{pump} , it is now the probe that is closer to resonance with the excited state and thus far more likely than the pump to excite the atoms sitting in the $|1,0\rangle$ state to the excited state (i.e., to the $|2,\pm1\rangle$ states) and then, by stimulated emission back into the probe, to the $|1,0\rangle$ state again. However, as shown in Fig. 3c, when ω_{probe} approaches the value $\omega_{pump} + \delta'$ the excited atoms are increasingly induced by the pump to make a stimulated emission into the pump beam and drop from $|2,\pm1\rangle$ to the $|1,\pm1\rangle$ ground states. This absorption from the probe and stimulated emission into the pump causes a loss in the transmitted probe power. Note that the probe loss is maximum when $\omega_{probe} = \omega_{pump} + \delta'$.

The difference in sizes of the probe-loss and probe-gain features at $\omega_{probe} = \omega_{pump} \pm \delta'$is straightforwardly explained by examining Fig. 3b and Fig. 3c. In case (b), when $\omega_{probe} < \omega_{pump}$, an atom that is transferred from $|1,0\rangle$ to the excited state by the pump has a choice of either making a stimulated emission back into the pump and dropping into the $|1,0\rangle$ state again, or making a stimulated emission into the probe and dropping into the $|1,\pm1\rangle$ states resulting in probe gain. Clearly, the strong pump dominates the stimulated emissions in this case thus limiting the amount of probe gain. On the other hand, in case (c), when $\omega_{probe} > \omega_{pump}$, an atom that is transferred from $|1,0\rangle$ to the excited state by the probe has a choice of either making a stimulated emission back into the probe and dropping into the $|1,0\rangle$ state again (resulting in neither probe loss nor gain), or making a stimulated emission into the pump and dropping into the $|1,\pm1\rangle$ states resulting in probe loss. Again, the strong pump dominates the stimulated emissions, this time resulting in a large probe loss.

In between, when $\omega_{probe} = \omega_{pump}$, neither ω_{probe} nor ω_{pump} are efficiently tuned to cause stimulated emission from the excited state to the $|1,\pm1\rangle$ states. As shown in Fig. 3d, both the pump and the probe are equally likely to excite the atom to the excited state ($|2,0\rangle$ for the pump and $|2,\pm1\rangle$ for the probe), and by stimulated emission into

themselves, back into the $|1,0\rangle$ state. Therefore, the transmitted probe beam shows neither gain nor loss.

Thus, measuring the frequency separation between the centers of the probe gain and loss features in Fig. 3a yields twice the value of δ' the relative light shift between the $|1,0\rangle$ state and the $|1,\pm1\rangle$ states (see Eq. (3)).

Fig. 4 shows plots of the measured relative light shift δ' as a function of the pump intensity for the case of magneto-optically trapped atoms and for optical molasses. The values of the pump intensity I, plotted along the x-axis in Fig. 4, need to be determined by a careful auxiliary measurement: We measure the total intensity (say, I_0) in the trapping beam just before it is split into the x, y, z MOT beams. Only 83% of this light remains just before entering the chamber owing to the beams' subsequent passage through beamsplitters, waveplates, and mirrors in its path. By measuring the individual intensities of the three trapping laser beams after they exit the vacuum chamber, and summing them to obtain their total intensity we determined that the pump intensity lost an additional 14% through the chamber, meaning a loss of 7% from the entry point until the midpoint of the chamber. Hence the intensity of the pump, when it first presents itself to the cold atoms is $0.83\,(0.93)\,I_0 = 0.77\,I_0$. In order to account for the retroreflected beams we note that after passing through the cold atom ball the pump traverses the far half of the chamber and window (losing another 7%), is retroreflected by a mirror and quarter-wave plate combination (we measured this to be an additional 2% loss), then traverses again through the window and half the chamber (losing 7% again) before it makes a second pass through the atoms. Thus the total pump intensity I seen by the atoms, and plotted along the x-axis in Fig. 4, is $[0.77 + 0.77\,(0.93)^2\,(0.98)]\,I_0 = 1.4\,I_0$. Note that these intensity measurements described above are made on just a small central portion of the 15 mm MOT beams that spatially overlaps with the focal spot of the probe beam at the location of the cold atom cloud.

In the case of the molasses the measured light shifts agree well with the theoretically predicted values. The error bars on the theoretical curve, shown on just the two end-points of the curve, reflect the fact that our pump detuning -2.5Γ has a maximum experimental uncertainty of $\pm0.25\Gamma$. To the best of our knowledge, this is the first time that the light shifts measured in cold atoms using Raman pump-probe spectroscopy have been shown to be consistent with theory, without any fitting parameters. To the best of our knowledge, this is the first time that the light shifts measured in cold atoms using Raman pump-probe spectroscopy have been shown to be consistent with theory, without any fitting parameters. Work [17] presents our preliminary data on observations of light shifts in cold ^{85}Rb atoms. However, the theoretical model presented in [17] is inaccurate. Further, there is no discussion in [17] of the role of Zeeman shifts in the experiment. We now discuss this role below.

In Fig. 4 the energy-level shifts measured for the MOT are consistently higher than the typical light shifts of

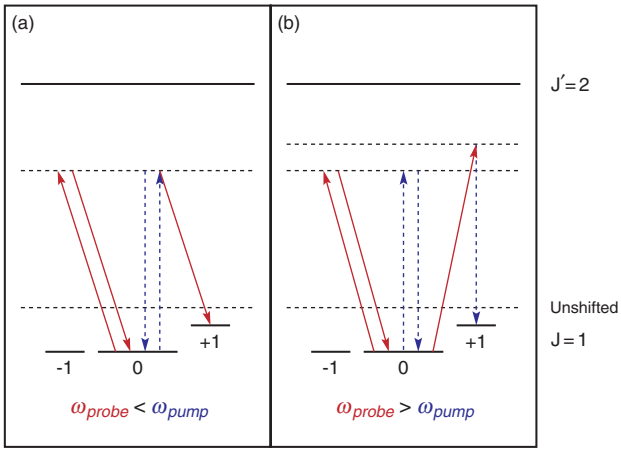

Figure 5 (online color at www.lphys.org) Role of the magnetic field gradient in probe transmission for (a) $\omega_{probe} < \omega_{pump}$ and (b) $\omega_{probe} > \omega_{pump}$, in the region of positive magnetic field. The probe (pump) is denoted by solid (dashed) lines. In the region of negative magnetic field the roles of the $|1,-1\rangle$ and $|1,+1\rangle$ states are interchanged, so the transmission spectrum is the same as in the positive region

~ 150 kHz observed for molasses. The presence of the magnetic gradient (12 G/cm in our case, as mentioned earlier) in the MOT imparts additional Zeeman shifts to the light shifted energy levels. To estimate the size of the Zeeman shift we note that the focal spot of the probe beam inside the 2.3 mm diameter cold atom cloud is 0.4 mm, which means that the magnetic field values seen by the cold atoms range from zero in the center up to ±0.24 Gauss at the edges of the cloud. The Zeeman shift between consecutive magnetic sub-levels of the $F = 3$ ground state of ^{85}Rb is known to be 0.47 MHz/G [18], implying that we may expect Zeeman shifts of up to 110 kHz. Thus one typically expects for the MOT a total energy level shift of about 260 kHz. This is close to the observed shifts in the MOT, as shown in Fig. 4. Indeed, the observed shifts are very slightly higher, most likely owing to residual dc magnetic fields. We use additional current coils in Helmholtz configuration to cancel the Earth's magnetic field and other stray dc magnetic fields acting on the cold atoms but, by our estimation, residual dc fields at the level of few tens of milliGauss persist.

Because the $|1,\pm1\rangle$ ground state sublevels tune in opposite directions with an applied magnetic field, one may at first glance expect that the Zeeman shifts would lead not to an increased value of δ' in Fig. 3a but, instead, to a broadening of the probe-gain and probe-loss features. We observed this, though, is not the case. Fig. 5 below explains why.

In the region of positive magnetic field the $|1,+1\rangle$ sublevel of our toy $J = 1 \rightarrow J' = 2$ atom is shifted upward, closer to resonance with the excited state and farther away from the unshifted $|1,0\rangle$ sub-level. On the other hand, the

$|1,-1\rangle$ sub-level is pushed downward, farther away from resonance with the excited state, close to the $|1,0\rangle$ sub-level. As shown in Fig. 5, this leads to a suppression of the role of the $|1,-1\rangle$ sub-level in the stimulated Raman pump-probe processes described in Fig 3b and Fig 3c. In Fig. 5a, where $\omega_{probe} < \omega_{pump}$, the dominant Raman process observable in the probe transmission spectrum is pump-photon absorption followed by probe-photon stimulated emission, leading to probe gain. The $|1,-1\rangle$ sub-level scarcely plays a role in the observable Raman processes because it lies closer to the $|1,0\rangle$ state leading to the situation described in Fig. 3d. Similarly, in Fig. 5b, where $\omega_{probe} > \omega_{pump}$, the dominant Raman process observable in the probe transmission spectrum is probe-photon absorption followed by pump-photon stimulated emission, which leads to probe loss. Again, the $|1,-1\rangle$ sub-level plays no role in observable Raman processes because it lies close to the $|1,0\rangle$ state as before. In the region of negative magnetic field, the roles of the $|1,+1\rangle$ and $|1,-1\rangle$ states are reversed.

In conclusion, we have measured the light shifts, also known as AC Stark shifts, as a function of laser intensity in cold ^{85}Rb atoms by observing gain and loss features in the transmission spectrum of a weak probe beam passing through the atoms. The observed gain/loss features are over an order of magnitude narrower than the natural linewidth. In the case of optical molasses the observed light shifts were found to be in good agreement with the theoretical values predicted by a simple model that we developed of a multilevel ^{85}Rb atom interacting with pump and probe beams. This is the first time that the light shifts in cold atoms measured as a function of intensity have been shown to be in agreement with a simple theory that has no free parameters. In the case of the MOT the observed energy level shifts were found to be consistently higher than those obtained for molasses. We have provided a simple explanation, based on Raman stimulated absorption and emission processes between light- and Zeeman-shifted energy levels, that yields predicted values of the total energy level shift which are in reasonable quantitative agreement with the observed level shifts for the MOT.

Acknowledgements We gratefully acknowledge invaluable discussions with Mr. Lynn Johnson in the Instrumentation Laboratory at Miami University. Financial support from the Petroleum Research Fund and the Research Corporation is gratefully acknowledged.

References

[1] G. Grynberg and C. Robilliard, Phys. Rep. **355**, 335 (2001), and references therein.
[2] T.M. Brzozowski, M. Brzozowska, J. Zachorowski, M. Zawada, and W. Gawlik, Phys. Rev. A **71**, 013401 (2005).
[3] M. Brzozowska, T.M. Brzozowski, J. Zachorowski, and W. Gawlik, Phys. Rev. A **72**, 061401 (2005).
[4] D. Grison, B. Lounis, C. Salomon, J.-Y. Courtois, and G. Grynberg, Europhys. Lett. **15**, 149 (1991).
[5] J.W.R. Tabosa, G. Chen, Z. Hu, R.B. Lee, and H.J. Kimble, Phys. Rev. Lett. **66**, 3245 (1991).
[6] J. Dalibard and C. Cohen-Tannoudji, J. Opt. Soc. Am. B **6**, 2023 (1989).
[7] Y.-C. Chen, Y.-W. Chen, J.-J. Su, J.-Y. Huang, and I.A. Yu, Phys. Rev. A **63**, 043808 (2001).
[8] J. Zachorowski, T. Brzozowski, T. Pałasz, M. Zawada, and W. Gawlik, Acta Phys. Pol. A **101**, 61 (2002).
[9] M. Schiavoni, Dynamique des Atomes Dans un Réseau Optique Dissipatif: Modes de Propagation, Résonance Stochastique, Diffusion Dirigée, Thèse de Doctorat de L'École Polytechnique (L'École Polytechnique, 2003), page 65.
[10] M.H. Shah, H.A. Camp, M.L. Trachy, G. Veshapidze, M.A. Gearba, and B.D. DePaola, Phys. Rev. A **75**, 053418 (2007).
[11] M. Brzozowska, T.M. Brzozowski, J. Zachorowski, and W. Gawlik, Phys. Rev. A **73**, 063414 (2006).
[12] J.A. Greenberg and D.J. Gauthier, Phys. Rev. A **79**, 033414 (2009).
[13] B. Deissler, K.J. Hughes, J.H.T. Burke, and C.A. Sackett, Phys. Rev. A **77**, 031604 (2008).
[14] V.I. Yukalov, Laser Phys. Lett. **1**, 435 (2004).
[15] S. Stock, B. Battelier, V. Bretin, Z. Hadzibabic, and J. Dalibard, Laser Phys. Lett. **2**, 275 (2005).
[16] H.J. Metcalf and P. van der Straten, Laser Cooling and Trapping (Springer-Verlag, New York, 1999).
[17] N.J. Souther, Light Shift Measurements of Cold Rubidium Atoms Using Raman Pump-Probe Spectroscopy, Master's thesis (Miami University, Oxford OH, USA, 2009).
[18] E. Arimondo, M. Inguscio, and P. Violino, Rev. Mod. Phys. **49**, 31 (1977).